Advances in Nano Research, *Vol. 10, No. 5 (2021) 461-470*
DOI: https://doi.org/10.12989/anr.2021.10.5.461

Synthesis and radiolabeling of PEGylated dendrimer-G_2-Gemifloxacin with ^{99m}Tc to Biodistribution study in rabbit

Naser Mohtavinejad[1a], Shaya Dolatshahi[2], Massoud Amanlou[**3], Mehdi Shafiee Ardestani[*4], Mehdi Asadi[3] and Ali Pormohammad[5]

[1]*Department of Radiopharmacy, Faculty of Pharmacy, Baqiyatallah University of Medical Sciences, Tehran, Iran*
[2]*Pharm, D. Faculty of Pharmacy, Tehran University of Medical Sciences, Tehran, Iran*
[3]*Department of Medicinal Chemistry, Faculty of Pharmacy, Tehran University of Medical Sciences, Tehran, Iran*
[4]*Department of Radiopharmacy, Faculty of Pharmacy, Tehran University of Medical Sciences, Tehran, Iran*
[5]*Department of Microbiology, School of Medicine, Shahid Beheshti University of Medical Sciences, Tehran, Iran*

(*Received June 7, 2020, Revised January 16, 2021, Accepted January 17, 2021*)

Abstract. Infection is one of the major mortality causes throughout the globe. Nuclear medicine plays an important role in diagnosis of deep infections such as osteomyelitis, arthritis infection, heart valve and heart prosthesis infections. Techniques such as labeled leukocytes are sensitive and selective for tracking the inflammations but they are not suitable for differentiating infection from inflammation. Anionic linear-globular dendrimer-G_2 was synthesized then conjugation to gemifloxacin antibiotic. The structures were identified by FT-IR, ^{1}H-NMR, C-NMR, LC-MS and DLS. The toxicity of gemifloxacin and dendrimer-gemifloxacin complex was compared by MTT test. Dendrimer-G_2-gemifloxacin was labeled by Technetium-99m and its in-vitro stability and radiochemical purity were investigated. In-vivo biodistribution and SPECT imaging were studied in a rabbit model. Identify and verify the structure of the each object was confirmed by FT-IR, ^{1}H-NMR, C-NMR and LC-MS, also, the size and charge of this compound were 128 nm and -3/68 mv respectively. MTT test showed less toxicity of the dendrimer-G_2-gemifloxacin than free gemifluxacin ($P < 0.001$). Radiochemical yield was > %98. Human serum stability was 84% up to 24 h. Biodistribution study at 50 min, 24 and 48 h showed that the complex is significantly absorbed by the intestine and accumulation in the lungs and affects them, finally excreted through the kidneys, biodistribution results are consistent with results from full image means of SPECT/CT technique.

Keywords: Technetium-99m; gemifloxacin; labeling; biodistribution; dendrimer-G_2

1. Introduction

In the beginning of 21st century, infection is still the cause of numerous cases of mortality throughout the world, and developing countries has paid a huge cost for that. The number of cases of multiple drug bacterial resistance and Tuberculosis reaches to a warning level, hence infection diagnosis, treatment and control are among the major challenges of science (Alavi and Zhuang 2001). Indeed, it is very essential to differential diagnosis between infection and inflammation. In this regard, radiolabeled antibiotics have privileges because many of the properties of the ideal infection-specific agent through antibiotics localizes in infection place (Lambrecht 2011). Moreover, detection of deep infections such as Peritonitis, Endocarditis and osteomyelitis is very difficult which could result in late diagnosis and treatment or even death in some cases (Das *et al*. 2002). Gemifloxacin is a wide spectrum synthetic antibiotic from the group of fourth generation Fluoroquinolones which affects gram positive and gram negative bacteria through inhibiting DNA-gyrase enzyme. This antibiotic has moderate to severe side effects which will be resolved by cutting drug administration (Sadeek *et al*. 2016, Blondeau and Tillotson 2007).

Recently, nanoparticles have been prepared to be used a carriers for drug delivery. Nanocarriers can improve the drug performance and reduce its side effects by changing its pharmacokinetics properties (Jain *et al*. 2019). Various substances such as polymers, metals and lipids have been employed for synthesis of nanoparticles for nanocarrier purposes (Madavan and Balaraman 2017). They can have different shapes and sizes depending on their synthesis methods (Raza *et al*. 2016). Nanocarrier-based drug delivery systems are now used in drug market and their application is increasing day by day. The future perspective of the researches on pharmaceutical nanoparticles is focused on development of nanosystems with multiple functions i.e. particles with capability of targeted drug delivery and imaging function (de Oliveira Freitas *et al*. 2017, Grant *et al*. 2019). One of this drug carrier is PEGylated dendrimer-G_2. Citric acid and polyethylene glycol provide dendrimers with flexibility and biocompatibility (Arima *et al*. 2017). Therefore, such dendrimers are healthy and non-toxic just like dendrimers

*Corresponding author, Associate Professor,
E-mail: Shafieeardestani@gmail.com
**Co-corresponding author, Professor,
E-mail: Amanlou@tums.ac.ir
[a]Ph.D., E-mail: Nasermohtavinejad@gmail.com

ISSN: 2287-237X (Print), 2287-2388 (Online)

obtained from biological blocks (Gothwal *et al*. 2020). The unique properties of dendrimers are due to their multi-branch structure, precise molecular weight, globular shape, internal pores, high permeability through cell membrane and low polydispersity. These features have resulted in high drug loading capability, high bioavailability and formation of a multi-functional scaffold applicable for both diagnostic and therapeutic purposes (Ghaffari *et al*. 2018). By modification of surface factors, the toxicity reduction and better targeting will be possible (Sonvico *et al*. 2018).

Although, radiological imaging such as X-ray, computerized tomography (CT), ultrasound and magnetic resonance imaging (MRI) are ordinarily used, but uses of these techniques are limited due to insignificant anatomical changes in the early stages of the infection process (Das *et al*. 2002, Lupetti *et al*. 2003). Single-photon emission computed tomography (SPECT) and positron emission tomography (PET) are two of the imaging techniques which can provide important information by showing the site of radiopharmaceutical accumulation (Li *et al*. 2018). For these techniques, various compounds are designed to be used as radiotracers. Among the variety of radionuclides used in nuclear medicine such as: ^{123}I, ^{111}In, ^{155}Tb, ^{18}F, ^{64}Cu, ^{68}Ga, ^{11}C, ^{13}N and ^{15}O, $TcO_4^-$is one of the most applicable radionuclide in radiopharmaceuticals (Farkas *et al*. 2016). ^{99m}Tc has found the highest diagnostic applications due to its especial nuclear properties (including its half-life, energy emission and possibility of its preparation in generator form) (Desmonts *et al*. 2020). In a study by Carvalho *et al*. (2013), ^{99m}Tc was introduced as a radioisotope which is capable of labeling nanoparticles. ^{99m}Tc imaging is a high sensitive imaging method which is more valuable than CT-scan technique, in this regard, further study on this radioisotope is highly recommended (Miyashita *et al*. 2019). In this regard, Karthikeyan *et al*. (2012) developed the use of dendrimers for Ciprofloxacin delivery. Ciprofloxacin-loaded dendrimers have substantial antibacterial properties. In this study, anionic linear-globular dendrimer-G_2 was synthesized then was conjugated to gemifloxacin antibiotic and labeled to ^{99m}Tc with high radiochemical purity. Afterwards it was injected to rabbit animal model for investigation of biodistribution.

2. Experimental

2.1 Reagents

All chemical reagents were of analytical grade and used without further purification. Polyethene glycol diacid 600 Da, citric acid, N, N'-Dicyclohexylcarbodiimide (DCC) and 1-Ethyl-3-(3-dimethylaminopropyl) carbodiimide (EDC) were provided from Merk (Darmstadt, Germany). An infrared spectrum was measured on Perkin Elmer Spectrum BX-II spectrometer. For FT-IR test, a thin tablet of nano-complex and KBr was prepared and the FT-IR spectra were recorded by Parkin Elmer spectrophotometer. The proton nuclear magnetic resonance (^{1}HNMR) spectra were measured in Chloroform-d (deuterochloroform, $CDCl_3$) by Bruker 500 MHz instrument (Billerica, Massachuset, Germany). LC-MC technique for PEGylated dendrimer-G_2 assay was also performed by means of Bruker (Germany). Gemifloxacin was purchased from Sigma-Aldrich Co. (St Louis, MO, USA). PEGylated dendrimer-G_2.Gemifloxacin was assessed by a liquid chromatography-mass spectrometry (LC-MS) analysis was provided by Agilent 6410 Triple Quadrupole LC-MS. Dynamic light scattering (DLS) procedure was conducted using the Malvern nano-zs, (Nano-ZSP, Malvern, UK). Atomic Force Microscopy (AFM) analysis was performed by JPK Nanowizard II.

Human embryonic kidney 293 (HEK-293) cells used for cytotoxic assays were purchased from the Pastor Institute (Tehran, Islamic Republic of Iran) and routinely grown in Roswell Park Memorial Institute (RPMI-1640) containing 10% FBS, amino acids, vitamins, and penicillin/streptomycin (Gibco, Eggenstein, Germany). In addition, Annexin-V FLOUS staining kit and XTT powder were purchased from Sigma Aldrich. Technetium-99m sodium pertechnetate ($Na^{99m}TcO_4$) was eluted from a commercial ^{99}Mo/^{99m}Tc-generator (Radioisotope Division, NSTRI, Tehran, Iran). Radiochemical purity (RCP) was monitored by silica gel thin-layer chromatography (SG-TLC) strips (silica gel 60; Merck). Quantitative gamma counting was conducted on an ORTEC model 4001 M γ-system well counter. Animal research was performed following the guidelines of animal care from the Committee of Tehran University of Medical Sciences (Number IR.Tums.REC.1394.1509). Planar and SPECT/CT imaging were acquired using Dual-head gamma camera (E.cam, Siemens, Germany).

2.2 Chemical synthesis of dendrimer-G_2 and conjugation by gemifloxacin

First, 2 mL of PEG600 (possessing 2 carboxyl groups in both sided) were collected and transferred to a 50-mL Erlenmeyer flask, then 5 mL DMSO was added as the solvent. 0.5 gr of N, N'-Dicyclohexylcarbodiimide (DCC) was measured by digital balance and added to the Erlenmeyer flask (as activator of surface functional groups to accelerate the reaction). In this step, the flask was capped and put on magnetic stirrer at temperature of 25°C and rate of 400 rpm for 15 min. Afterwards, 1 gr citric acid was added which acted as linker between the dendrimer and our desired molecule. The flask was again capped and stirred for further 2 h at the rate of 400 rpm. In this stage, dendrimer G_1 was synthesized. To producing dendrimer-G_2, 1 gr DCC, 1 gr citric acid were added to the solution (dendrimer G_1) and the solution was stirred at the rate of 400 rpm for a week at room temperature which resulted in formation of dendrimer-G_2. After 1 week, 5 mL distilled water and some amount of calcium chloride (for absorbing water) were added. The mixture was filtered by a dialysis membrane (cutoff 500-1,000 Da) to purify the reaction product against double distilled water for 24 h at ambient temperature, then the dialyzed product was subjected to a freeze-dried process.

Afterwards, dendrimers-G_2 was conjugated to gemifloxacin. Briefly, 0.05 g dendrimer-G_2 added to 10 mL of DMSO and 1 g DCC was added as an activator to the reaction solution. 10 min after getting stirred 1-mg

gemifloxacin were added. Then the flask was capped and stirred at the rate of 400 rpm for 1 week. Afterwards, 5 mL distilled water was added to the mixture for sediment the DCC. The solution was then poured in a dialysis bag and put in beaker containing 100 mL distilled water and stirred for 24 h. The water of the beaker was then replaced with new one and the dialysis bag (cutoff 500-1,000 Da) was stirred for further one hour. The content of dialysis bag was then transferred to 10-mL vials and sent to Pasture Institute for lyophilization. Size and charge of the nano-complex was determined by DLS technique through use of zeta size analyzer.

2.3 Radiolabeling PEGylated dendrimer-G2-gemifloxacin by ^{99m}Tc

The ^{99m}Tc-dendrimer-G_2 is similar to ^{99m}Tc-citrate, thus the square pyramidal structure of the complexes created by oxygen atoms at the surface (Magneson *et al*. 2016). To reach the high radiochemical purity we have examined different parameter containing (i) altering the amount of ligand (PEGylated dendrimer-G_2-gemifloxacin), (ii) different volume of $SnCl_2$ as a reducing agent (iii) adjusting of different PH and (iv) watching the different reaction time and temperature.

2.4 Radiochemical purity

The radiochemical yield of ^{99m}Tc-nanoconjugate was measured by Whatman 2 strips (1.2 × 10 cm) as solid phases in two different mobile phases: acetone: methanol (1:1) for free $^{99m}TcO_4^-$ impurity (R_f = 1.0) and normal saline 0.9% for ^{99m}Tc colloid impurity (R_f = 0.0) (Mohtavinejad *et al*. 2020). In acetone: methanol (1:1) is used as a mobile phase, the labeled nanoconjugate remained at the origin (R_f = 0), while ^{99m}Tc-nanoconjugate move with normal saline 0.9% (R_f = 1). Then, the strips (10 cm) were cut into 1 cm parts and the radioactivity of each segment was quantified in a gamma-type well counter. RCP was calculated through the following relation:

RCP = 100 - (free ^{99m}Tc pertechnetate + $^{99m}TcO_2$)

2.5 Serum stability and partition coefficient (Log P) test

The ^{99m}Tc-dendrimer-G_2-gemifloxacin with 30 MBq activity was added to 1 mL of human serum. After incubation of the tracer at 37°C, at the time of testing, 100 µL of trichloroacetic acid 10% was added to the mixture and serum were precipitated by centrifugation. Sampling was performed at 1-, 2-, 4- and 24-hour intervals. Then, the radiochemical purity was calculated by Whatman-2 strips. To assess partition coefficient, 25 MBq of radiolabelled complex in 0.5 mL n-octanol and 0.5 mL phosphate buffer saline were added to a 2 mL micro-tube. The micro-tube was shaken by a mechanical shaker and mixing time was set over a period of 10 min. Phase split was performed by centrifuging at 5,000×g for 5 min. Then, 100 µL solution of each phase was taken and radioactivity was counted using a γ well-type counter. By the following relation Log P was calculated:

Log P = log {radioactivity in n-octanol / radioactivity in normal saline}

2.6 Cytotoxicity evaluations

Cytotoxicity evaluations was prepared as described previously (Mohtavinejad *et al*. 2020). In summary, XTT (2,3-Bis-(2-methoxy-4-nitro5-sulfophenyl)-2H-tetrazolium-5-carboxanilide salt) assay was employed to investigate the toxicity of nano-conjugates. This method is based on investigating dehydrogenase enzyme in living cells. The reaction demands the presence of an electron coupling reagent, which is PMS (N-methylphenazonium methyl sulfate), working as an intermediate electron acceptor and can considerably increase the XTT reduction efficiency in cells. The HEK-293 cells were seeded with 10.000 cells per well in a 96-well plate and were incubated by dendrimer-gemifloxacin nano-conjugates and gemifloxacin in four concentrations of 100, 200, 300 and 400 µg/mL for 48 h. After 48 h, XTT/PMS (50/1 µL) reagent was added to the samples for 3-4 h, the results were read by ELISA plate reader in a wavelength of 450 nm.

2.7 Biodistribution studies

Biodistribution was done with generally accepted guidelines governing animal work. The Male New Zealand White rabbits weighting 2~2.5 kg randomly chose this work. First rabbits were anaesthetized by the intramuscular given of ketamine, then 400 µL of the solution including 200 MBq of the ^{99m}Tc-nanoconjugate was injected into the marginal ear vein. Rabbits were euthanized at time intervals of 50 min, 24 h and 48 h after injection after inoculated ketamine, then different organs including kidneys, bone, muscle, salivary glands, heart, kidneys, bone, muscle, spleen and intestines were removed and rinsed with saline solution to clean their residues blood. Also, to assess the radioactivity in blood, it was obtained from the heart by syringes containing heparin. The same moment counter-weight and the radioactivity counted in the gamma counter. The percentage of the injected dose per gram (% ID/g) was measured for all tissue.

2.8 Scintigraphy studies

^{99m}Tc-PEGylated dendrimer-G_2-gemifloxacin (200 MBq, 400 µL) was injected via a marginal ear vein in rabbits to evaluation of pharmacokinetic by SPECT imaging. Instantly, rabbits were anaesthetized by intramusscels injecting of ketamine and images by SPECT/CT that equipped with low energy high-resolution collimators, a 256*256 matrix size and a 20% energy window set at 140 keV were performed. The images were taken 50 min, 24 h and 48 h after injection.

2. Statistical analysis

Data from at least three trials was expressed as mean ±

SD. The student's t-test was used to analyze the treatment results and that of the control experiment. The calculations of means and standard deviations for biodistribution were performed on Prism-Graph Pad (2018). A two-sided p-value of less than 0.05 was considered statistically significant. For comparison of the data from different groups, one way ANOVA test was employed.

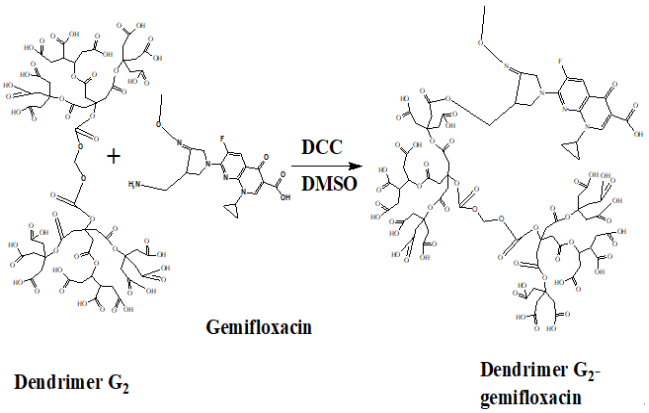

Fig. 1 schematic illustration of dendrimer-G_2 synthesis and conjugation to gemifloxacin

3. Results

3.1 Characterization of dendrimer-gemifloxacin conjugate

Synthesis of the dendrimer-G_2 and the gemifloxacin conjugation process have been described earlier. Fig. 1 shows schematic illustration of dendrimer-G_2 synthesis and conjugation of gemifloxacin to the dendrimer. On general, the stages were as follows: The amine groups of gemifloxacin react with carboxylic acid groups of dendrimer and these two molecules will be attached to each other by amide bonds. To confirm the linkage between dendrimer-G_2 and gemifloxacin, FT-IR, CNMR, HNMR, LC-MC and FT-IR techniques were employed.

FT-IR spectra of dendrimer-gemifloxacin is shown in Fig. 2(a). The peaks related to gemifloxacin-dendrimer conjugation amide bond were indicated by two sharp peaks at 3327.85 cm^{-1} (due to N-H) and 1685.35 cm^{-1} for amid C=O bonds; while the peaks in 2929.73 cm^{-1} are attributed to aliphatic CH and CH_2 bonds. The Golden Peak for the detection of the presence of gemfloxacin in final product is C-F, which appeared in 1058.4 cm^{-1}. On the Noncomplex ^{1}H-NMR was investigated in DMSO-d_6 as solvent and

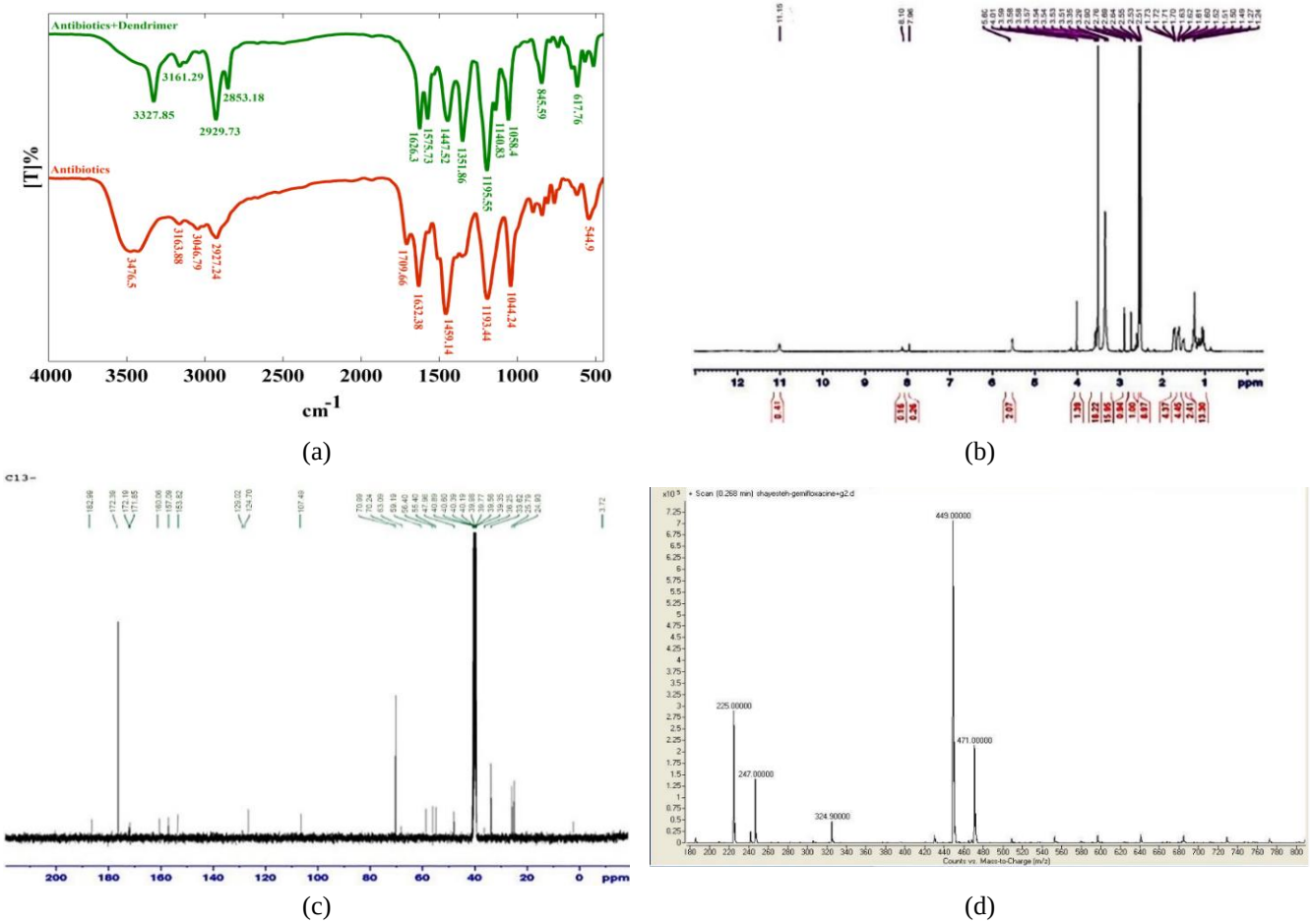

Fig. 2 (a) FT-IR spectroscopy of dendrimer G_2-gemifloxacin conjugation; (b) ^{1}H-NMR spectrum of dendrimer G_2-gemifloxacin conjugation; (c) CNMR spectroscopy of dendrimer G_2-gemifloxacin conjugation and; (d) LC-Mass spectroscopy dendrimer G_2-gemifloxacin conjugation

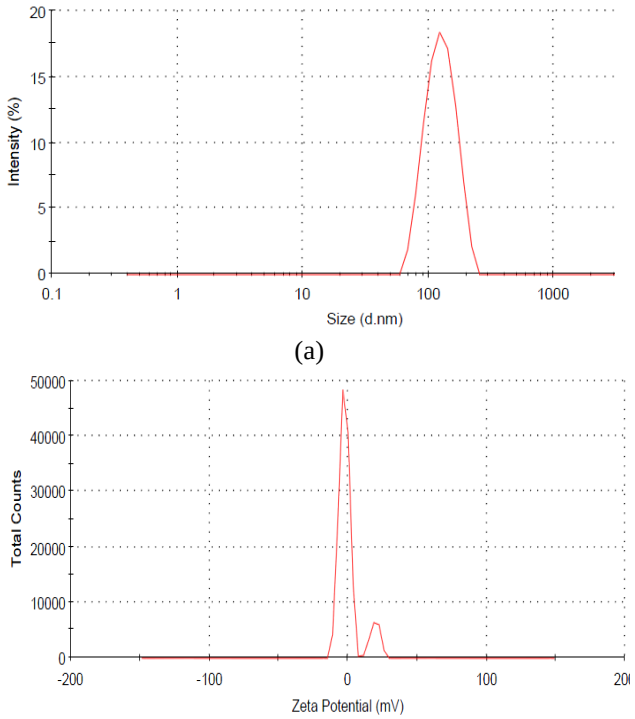

(a)

(b)

Fig. 3 (a) Size and (b) Zeta potential. Red colors show the dendrimer G2-gemifloxacin nanoparticles

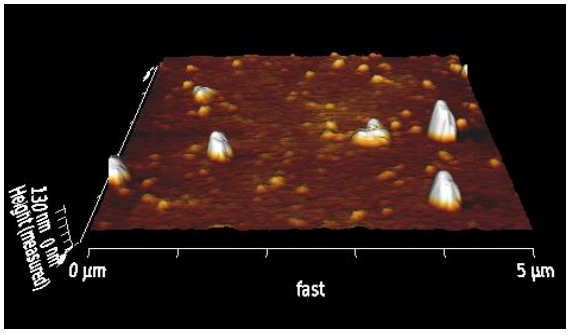

(a)

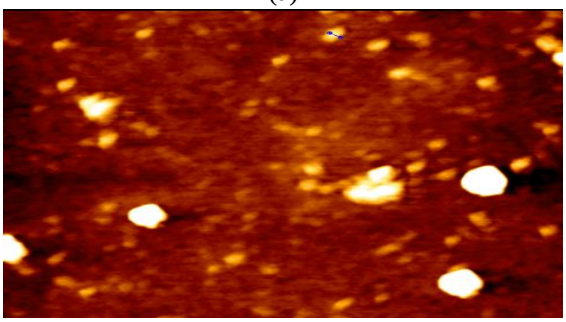

(b)

Fig. 4 Atomic force microscopy image of the dendrimer G2-gemifloxacin nanoparticles nanoconjugate

using a 500 MHz bucker, in which the singlet peak at 11.05 ppm was associated with the acidic hydrogen of the gemfloxacin structure, which is considered the most Deshields peak product. After that, the presence of a small peak in 7.96 ppm, is related to the amide group which this peak is confirms the linkage of gemifluxacin and

Table 1 Effect of pH on the radiolabeling efficiency of ^{99m}Tc- dendrimer G_2-gemifloxacin nanoparticles (mean ± SD, n = 3)

pH	Radiochemical purity (%)
5	68.1 ± 2.2
6	70.5 ± 3.2
6.5	73.9 ± 5.1
7	85.2 ± 3.1
7.4	94.5 ± 3.1
8	97.1 ± 1.3
8.3	98.1 ± 1.6

dendrimer. The singlet peak in 5.60 ppm is related to methylene between carbonyl and oxygen group (-O-**CH**$_2$-CO-). The single peak at 4.01 ppm can be clearly identified from its chemical shift as being the N-CH_2 peak in imidazoline ring and strong peak at 3.56 ppm, it shows methyl group's protons. Furthermore, the peaks related to methylene beside to oxygen (CH_2-**CH**$_2$-O) or carboxylic acid (**CH**$_2$COO) groups, were illustrated in 3.8 ppm as triplet and in 2.8 ppm as doublet-doublet peak respectively. Finally, other methylene and methane residue from cyclopropane group in the gemifluxacin, and dendrimer structure is represented in 1.24-173 ppm that confirm the the linkage of gemifluxacin and dendrimer Fig. 2(b). In the ^{13}C-NMR graph of sample, the presence of poor peak in 3.8 and 36.2 ppm is related to cyclopropane ring. Low intensity of these peaks indicate that they are less abundant than other carbons in the sample structure. Furthermore, ten aliphatic carbon types are presented in 24.8-70.2 ppm and seven aromatic carbon types are illustrated in 107.5-161.0 ppm. At last, amidic, steric, acidic and ketones carbons are appeared in 171.0, 172.2, 177.3, 183.0 ppm respectively. a long and distinct peak in the area of 40 is associated with the CH_2 alphabet, a tallish peak in region of 78 is related to the core of PEG dendrimer and tall peak in 187 is related to carbonyl that confirm the presence of our two compounds in the complex Fig. 2(c). LC-MS spectra are presented in Fig. 2(d). According bell-shaped structure of 808 m/z, 772 m/z and 684 m/z break indicates units of CH_2-CH_2 in PEG along with a citric acid group repetitively. Therefore, presence of dendrimer-G_2 can be verified in nano-conjugate. Moreover, existence of two high and sharp peaks at 449 m/z and 225 m/z confirmed conjugation of gemifloxacin to dendrimer-G_2.

3.2 Conjugate size, zeta potential and AFM

According to a study we did before (Mohtavinejad *et al.* 2020), size and zeta potential of non-conjugated dendrimer was 93 nm and -3.2 mV. The structure and size distribution of dendrimer-gemifloxacin was also investigated and verified by zeta size analyzer. Based on Fig. 3(a), the presence of gemifloxacin can be proven with increasing size. The average size and zeta potential of the nano-conjugate were 128 nm and -3.68 mV respectively, Figs. 3(a)-(b). Therefore, according to the obtained graphs, more

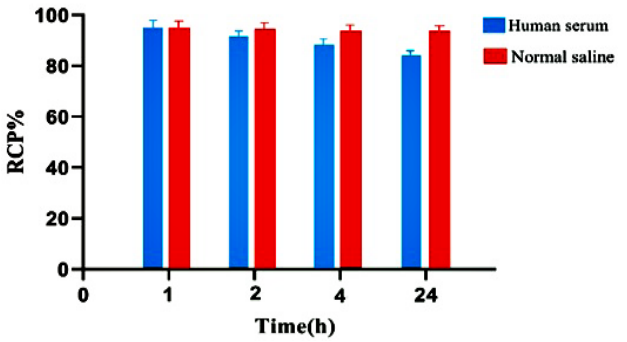

Fig. 5 Serum and normal saline stability of ^{99m}Tc-dendrimer G_2-gemifloxacin

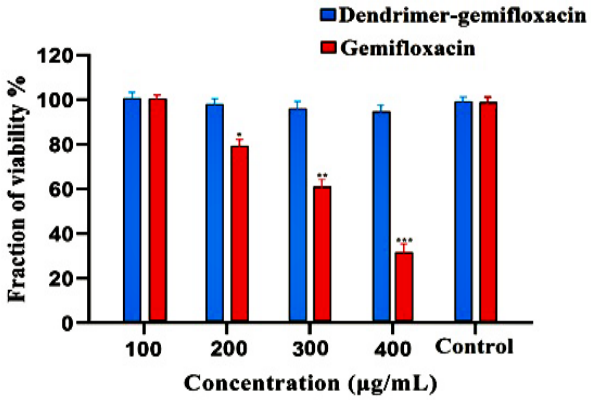

Fig. 6 MTT assay: HEK-293 cells were exposed to the nanoconjugate for 48 h (n = 3, *P < 0.05, **P < 0.01 and ***P < 0.001 for 48 h)

Table 2 Biodistribution of ^{99m}Tc-dendrimer G_2-gemifloxacin nanoparticles in normal rabbits (% injected dose per gram organ ± SD, n = 3)

Organ	50 min	24 min	48 min
Blood	1.18 ± 0.31	0.16 ± 0.22	0.06± 0.31
Heart	1.28 ± 0.98	1.8 ± 0.42	0.09 ± 0.66
Lung	0.56 ± 0.16	5.24 ± 0.48	0.81 ± 0.52
Liver	4.31 ± 0.14	2.32 ± 0.31	1.94 ± 0.71
Spleen	2.22 ± 0.41	3.79 ± 0.12	1.05 ± 0.32
Stomach	0.86 ± 0.95	3.58 ± 0.01	4.31 ± 0.39
Intestines	10.01 ± 0.19	4.81 ± 0.68	0.91 ± 0.05
Kidneys	4.21 ± 0.32	15.30 ± 0.09	3.76 ± 0.03
Muscle	0.77 ± 0.12	0.22 ± 0.24	0.04 ± 0.21
Thyroid and Salivary gland	0.92 ± 0.61	0.21 ± 0.32	0.02 ± 0.84
Bone	0.75 ± 0.91	0.14 ± 0.31	0.04 ± 0.09

changes in charge and size of the conjugated compound can be regarded as a confirmation of the presence of gemifloxacin. Atomic force microscopy (AFM) as a very-high-resolution type of microscopic scanning probe, which demonstrates resolution on the order of fractions of a nanometer, was used for topographic imaging analysis gemifloxacin-conjugated anionic dendrimer-G_2. AFM image of the gemifloxacin-conjugated anionic dendrimer-G_2 was 130 nm, Fig. 4. Many studies have shown that the biodistribution and interaction of nanoparticles with cells can be affected by particle shape. Also, Fig. 4 contains confirmatory and supplementary information related to Fig. 3(a).

3.3 Radiolabeling of PEGylated dendrimer-G_2-gemifloxacin with ^{99m}Tc

To improve the efficiency of radiolabeling, a series of various labeling factors was studied. When the dendrimer as chelators was used, pH changes was most effective in radiochemical purity. Radiochemical yield was lower than 85% in pH 7, but it was more than 97% in pH 8, Table 1. Eventually, a radiochemical purity of > 98% was reached in a mixture of 100 µg dendrimer-G_2-gemifloxacin and 60 µg $SnCl_2$, pH>8.3 in normal saline as a solvent at 60°C. It should be noted ^{99m}Tc oxidation state in this complex is +5. A pyramidal structure is formed due to the binding of $^{99m}Tc^{5+}$ to the oxygen citrate atoms.

3.4 Serum stability and lipophilicity assessment

Beside on our research on human serum, about 84% stability of ^{99m}Tc-dendrimer-G_2-gemifloxacin within 24 h was seen. In comparison, in the same time, stability in normal saline solution was 93%, Fig. 5. $^{99m}TcO_4^-$ release from nano-complex was lower than 4% at 4 h; therefore, an appropriate and steady ^{99m}Tc-nanoconjugate was attained in human serum and normal saline. In addition, rate of ^{99m}Tc-dendrimer-G_2-gemifloxacin log P (lipophilicity) was -0.44.

3.5 MTT results

Since cell culture and passage, HEK-293 cell line was used for the XTT experiment. As the graph obtained from MTT assay test of dendrimer G_2-gemifloxacin and gemifloxacin shows, the cytotoxicity on healthy HEK-293 cells is far lower for the conjugated system as compared with gemifloxacin alone Fig. 6. A significant difference can be observed between dendrimer-gemifloxacin and gemifloxacin at concentration of 400 µg/mL (P < 0.001).

3.6 Biodistribution of ^{99m}Tc-dendrimer- gemifloxacin

Our biodistribution evaluation results about ^{99m}Tc-dendrimer-G_2-gemifloxacin in normal rabbit hypoxic model has given in Table 2. In the first 50 min, radio-nanoconjugate accumulation in the salivary gland, stomach, muscle and bone was insignificant. Since the thyroid and salivary glands are the critical organs for free- ^{99m}Tc, therefore, obtained data indicate in-vivo high radiochemical purity. Also, calculation of the Kidneys percentage of injected dose per gram (15.30 % ID/g in 24 h), we have seen main excretion rout of radiotracer over a period of time is through in these organs. With the passage of time accumulation of radiotracer in the liver was a decrease (4.31, 2.32, 1.94 %ID at 50 min, 24 and 48 h, respectively). This indicates the dendrimer metabolism and Hepatic-biliary tract as second exertion pathway of the radiotracer.

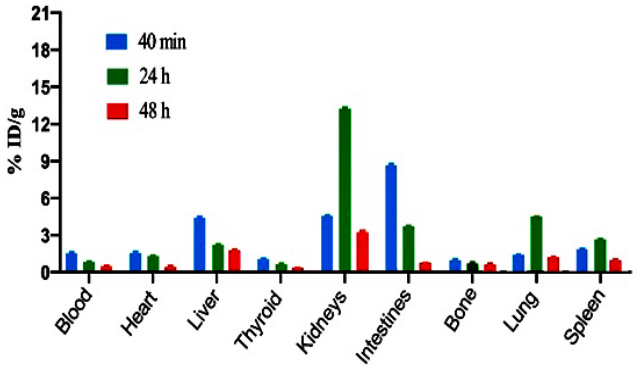

Fig. 7 comparison of biodistribution of ^{99m}Tc- dendrimer G_2-gemifloxacin nanoparticles in different organs 50 min, 24 h and 48 h after injection

Table 3 ^{99m}Tc-gemifloxacin biodistribution reported results in normal rabbit (% injected dose per gram organ ± SD, n = 3)

Organ	1 h	2 h	4 h
Liver	3.26 ± 0.11	2.97 ± 0.13	0.81 ± 0.15
Spleen	2.70 ± 1.1	1.65 ± 0.91	1.05 ± 0.32
Kidneys (RT)	2.39 ± 0.20	3.27 ± 0.12	3.76 ± 0.03
Kidneys (LT)	0.26 ± 0.08	2.99 ± 0.18	1.12 ± 0.23
Urinary bladder	31.07 ± 0.45	46.77 ± 0.42	61.78 ± 0.33
Bone	2.58 ± 0.20	1.49 ± 0.17	0.53 ± 0.07

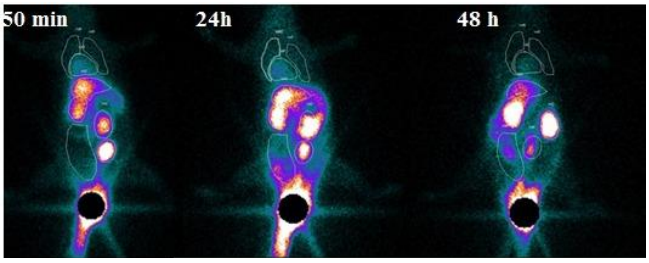

Fig. 8 SPECT scintigraphy of ratbody acquired at 50 min (A), 24 h (B) and 48 h (C) after injection

^{99m}Tc-gemifloxacin biodistribution reported results in normal rabbit showed that kidneys have the most uptake and urinary bladder is the main route of medicine excretion that is similar to our biodistribution result, Table 3 (Shahzad *et al*. 2019). One of the main problems with dendrimer compounds is self-aggregation during radiolabeling. The uptake amount of radiotracer in lung tissue was 0.56 ID/g at 50 min post-injection, which confirms the non-aggregation of dendrimer during radiolabeling, Fig. 7.

3.7 SPECT imaging (in vivo study)

SPECT scan in the normal rabbit model was taken at different time (50 min, 24 h and 48 h) after injection of 200 MBq of the ^{99m} Tc-dendrimer-gemifloxacin to assess the pharmacokinetic of the radiotracer as a new agent of gemifloxacin, Fig. 8.

4. Discussions

Nuclear medicine techniques (such as SPECT imaging) have found considerable application in diagnosis of different disease due to use of low concentration (nano or Pico molar), low half-life of radionuclides and therefore lower toxicity (Govaert *et al*. 2016). Throughout past 40 years, a small group of radiopharmaceuticals has been developed for diagnostic imaging purposes among patients suffering from infection or inflammation. These molecules usually contribute in immune response to antigens by linking with leukocytes or other immune system-related molecules (Torres *et al*. 2018, Pakos *et al*. 2007). In nuclear medicine, diagnosis of inflamed or infected region is under development. Huge efforts have been devoted for application of radiopharmaceuticals in inflammation diagnosis or resolving the infection (Signore and Glaudemans 2011). Recently, the non-cellular labeling tracers are used for this aim, such as ^{111}In–IgG, ^{67}Ga–citrate, ^{99m}Tc–nanocolloid, ^{99m}Tc–HIG, ^{99m}Tc–BW250/183 antibody, etc (Yurt *et al*. 2008, Mäkinen *et al*. 2005). Small molecules offer considerable advantages over immune-globulins or antibodies in the field of radiopharmaceuticals because of lack of immunogenicity, low uptake of reticuloendothelial organs such as liver and spleen and fast clearance from non-target tissues and blood (Okarvi 2004). Therefore, radiolabeled antibiotics received more attention due to the selective toxicity, may make a differential diagnosis between infection and sterile inflammation and the localizing tracer for infective area (Benitez *et al*. 2006).

In this study, anionic linear-globular dendrimer-G_2 was synthesized then was conjugated to gemifloxacin antibiotic and labeled to ^{99m} Tc. Among the radionuclides used in nuclear medicine, ^{99m}Tc has found a substantial application in nuclear medicine and pharmacy. Gamma energy of about 140 KeV of this radioactive element can be easily detected and owing to its low physical and biological half-life, it can be rapidly removed from body after imaging process. Single energy and purity of gamma radiation of this element are among the other advantages of this element (Kung *et al*. 1997). About 90% of imaging single energy photon-based radiopharmaceuticals includes this element (Das *et al*. 2002). In this framework, the first radiolabeled antibiotic to be established as a radiotracer was ^{99m}Tc-ciprofloxacin and it has been used quite extensively studied in humans (Solanki *et al*. 1993). Hall *et al*. (1998) in a similar study was developed ^{99m}Tc-ceftizoxime and it is shown maximum uptake for septic abscess at 1 h. Also, ^{99m}Tc-ceftizoxime is able to differentiate sterile inflammation from infection. Roohi *et al* (2005) was reported higher uptake of ^{99m}Tc-vancomycin and ^{99m}Tc-kanamycin in S. aureus infected foci (Roohi *et al*. 2006).

Regarding development of nanoscience and application of nanoparticles in drug delivery, researches on nanocarriers has attracted considerable attention. Among the nano-particles, dendrimers has found substantial application regarding to their single part and high functional groups (Jain *et al*. 2019). Among the dendrimers, polyamides and polyamines, PAMAM and polypropyleneimene (PPI), dendrimers possessing anionic tail groups has drawn

considerable attention due to their lower toxicity (Madavan and Balaraman 2017). In this research, first dendrimer G_1 was prepared through reaction of di acid polyethylene glycol with citric acid in DSMO at the presence of DCC which by addition of citric acid at the presence of DCC and purification by dialysis bag resulted in synthesis of dendrimer G_2 with efficiency of 94%. Anionic dendrimer G_2-gemifloxacin conjugate was obtained with efficiency of 89% by reaction of gemifloxacin solution with anionic dendrimer G_2 in DMSO at the presence of DCC and solution purification by dialysis bag. Structure of this gemifloxacin-conjugated anionic dendrimer-G_2 was confirmed though LC-MS, FT-IR, HNMR and CNMR spectra. According to recorded FT-IR spectrum, stretching vibration of N-H bond and C-H bond can be observed in 1626.3 and 2929.73 cm^{-1}, respectively. Breaks in LC-MS spectra reflect the synthesis of the desired compound. In a study, citric acid dendrimer with poly ethylene glycol core was used as an effective carrier for delivery of Minocycline. Encapsulation of Minocycline inside the dendrimer resulted in enhanced solubility and its higher activity in comparison with Minocycline alone (Sharma *et al*. 2017). Due to reaction with functional groups of molecules, dendrimers can carry them and reduction of drug dose by use of dendrimers will result in lower drug resistance and side effects. Dendrimers can also stabilize the chemical molecules and increase drug uptake of the cells. These molecules are capable of inhibiting HIV virus in the infected cells by linking with genes and transferring to the target cell (Alnasser *et al*. 2018).

After confirmation of gemifloxacin conjugation with dendrimer-G_2, the new eluted ^{99m}Tc was reduced from ^{99m}Tc (V) to ^{99m}Tc (IV) by 60 µL of $SnCl_2$ in 0.1 HCl and formed a complex with gemifloxacin-dendrimer. In this research, we used dendrimers as $^{99m}TcO_4^-$ chelator. According to Magneson and Orahood (2016) the feasible complex formed between $^{99m}TcO_4^-$ and dendrimer-G_2 in ^{99m}Tc-dendrimer-gemiflouxacin is Tc^{+5}. Our results showed RCP was more than 98%. Moreover, the results of another study, which used citric acid dendrimer-G_2 with conjugated methionine ^{99m}Tc-radiolabeled, showed that high RCP and this targeted dendrimer has high collection in adenoma cancerous cells of human colon carcinoma (Khosroshahi *et al*. 2013).

Studies show that the size and charge of the nanoparticles play an important role in the biodistribution and pharmacokinetic effects. Dendrimer-G_2-gemifloxacin size and charges were determined as 128 and -3.68, respectively. AFM image of the sample also confirmed the size and morphology of gemifloxacin-conjugated anionic dendrimer G_2. Viability percentage of HEK-293 cells exposed to synthesized conjugates was examined by MTT assay. One way ANOVA and Tukey's statistical tests showed that there is no statistically significant difference in cells viability of the test groups and control sample. In concentrations of 300 and 400 µg/mL, significant toxicity was observed with gemifloxacin. Our results showed that gemifloxacin-conjugated dendrimer is safer up to 400 µg/mL. In line with our investigation, has shown polyethylene glycol-dendrimer can decreases toxicity and enhances solubility by neutralizing their surface charges. This component also declines the clearance of dendrimer and increases its biocompatibility (Jain *et al*. 2019, Madavan and Balaraman 2017). Human serum stability assay in different time interval showed that ^{99m}Tc-dendrimer-G_2-gemifloxacin has appropriate stability (94% at 4 h vs 98% 1 min). On the other hand, in biodistribution study insignificant activity uptake of thyroid and salivary gland confirm the results of nano-complex serum stability test.

The data of biodistribution in rabbit showed that ^{99m}Tc-radiolabeled gemifloxacin-dendrimer has significant accumulation in intestine 50 min after injection reflecting the major path of up-taking this nano-complex. Mainly, fluoroquinolone antibiotics are metabolized in the liver and eliminated by renal excretion (Gomes *et al*. 2017). Furthermore, its significant accumulation of nano-complex in kidneys and liver indicates that the main way of metabolism and excretion pathways. Dendrimer and gemifloxacin are both hydrophilic and it is another reason to high activity uptake of kidneys. Planar SPECT imaging of rabbit at 50 min, 24 and 48 h post-injection revealed that ^{99m}Tc-radiolabeled gemifloxacin-dendrimer accumulated in various tissues. High activity of kidneys reflects that the main way of excreting and hydrophilicity of nano-complex. The results of SPECT scan have complete accordance with the results obtained from biodistribution.

5. Conclusion

Results obtained in this study revealed that the PEG dendrimer-G_2 was synthetized and conjugated to the gemifloxacin with high purity.

- The nano-complex structure were confirmed by FT-IR, ^{1}HNMR, CNMR and LC-Mass.
- Chelator-free radiolabeling of dendrimer with ^{99m}Tc was performed with high-yield and stable complexes.
- MTT assay revealed labeled nanoconjugate up to 400 µg/mL has no cellular toxicity.
- Biodistribution studies showed a higher uptake in the kidneys tissue in comparison to other organs.
- The main route of excretion was the urinary tract.
- The present results may provide a potential application of the radiolabeled nanostructure in the development of SPECT infection imaging.

Acknowledgments

The authors are grateful to the Research Council of Tehran University of Medical Sciences, Tehran, Iran for financial supports.

Conflict of Interest

The authors declare that there are no conflicts of interest.

References

Alavi, A. and Zhuang, H. (2001), "Finding infection-help from PET", *The Lancet*, **358**(9291), 1386. https://doi.org/10.1016/S0140-6736(01)06491-1.

Alnasser, Y., Kambhampati, S.P., Nance, E., Rajbhandari, L., Shrestha, S., Venkatesan, A., Kannan, R.M. and Kannan, S. (2018), "Preferential and increased uptake of hydroxyl terminated PAMAM dendrimers by activated microglia in rabbit brain mixed glial culture", *Molecules*, **23**(5), 1025. https://doi.org/10.3390/molecules23051025.

Arima, H., Motoyama, K. and Higashi, T. (2017), "Potential use of cyclodextrins as drug carriers and active pharmaceutical ingredients", *Chem. Pharm. Bull.*, **65**(4), 341-348. https://doi.org/10.1248/cpb.c16-00779.

Benitez, A., Roca, M. and Martin-Comin, J. (2006), "Labeling of antibiotics for infection diagnosis", *Q J Nucl. Med. Mol. Im.*, **50**(2), 147-52.

Blondeau, J.M. and Tillotson, G. (2007), "Gemifloxacin for the management of community-acquired respiratory tract infections", *Antibiotiques*, **9**(3), 173-180. https://doi.org/10.1016/S1294-5501(07)91376-X.

Carvalho, B.F., Albernaz, M.S. (2013), "Development of nanoradiopharmaceuticals by labeling polymer nanoparticles with tc-99m", *World J. Nucl. Med.*,**12**(1), 24-26. https://doi.org/10.4103%2F1450-1147.113946.

Das, S.S., Hall, A.V., Wareham, D.W. and Britton, K.E. (2002), "Infection imaging with radiopharmaceuticals in the 21st century", *Braz. Arch. Biol. Techn.*, **45**(SPE), 25-37. http://doi.org/10.1590/S1516-89132002000500005.

De Oliveira Freitas, L.B., de Melo Corgosinho, L., Faria, J.A.Q.A., dos Santos, V.M., Resende, J.M., Leal, A.S., Gomes, D.A. and de Sousa, E.M.B. (2017), "Multifunctional mesoporous silica nanoparticles for cancer-targeted, controlled drug delivery and imaging", *Micropor. Mesopor. Mat.*, **242**, 271-283. https://doi.org/10.1016/j.micromeso.2017.01.036.

Desmonts, C., Bouthiba, M.A., Enilorac, B., Nganoa, C., Agostini, D. and Aide, N. (2020), "Evaluation of a new multipurpose whole-body CzT-based camera: Comparison with a dual-head Anger camera and first clinical images", *EJNMMI physics*, **7**(1), 1-16. https://doi.org/10.1186/s40658-020-0284-5.

Farkas, R., Siwowska, K., Ametamey, S.M., Schibli, R., van der Meulen, N.P. and Müller, C. (2016), "64Cu-and 68Ga-based PET imaging of folate receptor-positive tumors: Development and evaluation of an albumin-binding NODAGA–folate", *Mole. Pharmaceutics*, **13**(6), 1979-1987. https://doi.org/10.1021/acs.molpharmaceut.6b00143.

Ghaffari, M., Dehghan, G., Abedi-Gaballu, F., Kashanian, S., Baradaran, B., Dolatabadi, J.E.N. and Losic, D. (2018), "Surface functionalized dendrimers as controlled-release delivery nanosystems for tumor targeting", *Eur. J. Pharm. Sci.*, **122**, 311-330. https://doi.org/10.1016/j.ejps.2018.07.020.

Gothwal, A., Malik, S., Gupta, U. and Jain, N.K. (2020), "Toxicity and biocompatibility aspects of dendrimers", *Pharmaceut. Applicat. Dendrimers*, **55**(11), 251-274. https://doi.org/10.1016/B978-0-12-814527-2.00011-1.

Govaert, G.A.M. and Glaudemans, A.W. (2016), "Nuclear medicine imaging of posttraumatic osteomyelitis", *Eur. J. Trauma. Emergency Surg.*, **42**(4), 397-410. https://doi.org/10.1007/s00068-016-0647-8.

Grant, J., Naeim, M., Lee, Y., Miya, D., Kee, T. and Ho, D. (2019), "Engineering multifunctional nanomedicine platforms for drug delivery and imaging", In: *Nanotheranostics for Cancer Applications*, pp. 319-344, Springer, Cham. https://doi.org/10.1007/978-3-030-01775-0_14.

Hall, A.V., Solanki, K.K., Vinjamuri, S., Britton, K.E. and Das, S.S. (1998), "Evaluation of the efficacy of ^{99m}Tc-Infecton, a novel agent for detecting sites of infection", *J. Clin. Pathol.*, **51**(3), 215-219. http://doi.org/10.1136/jcp.51.3.215.

Jain, S., Krishna Cherukupalli, S. and Mahmood, A. (2019), "Emerging nanoparticulate systems: Preparation techniques and stimuli responsive release characteristics", *J. Appl. Pharm. Sci*, **9**(8), 130-143. https://doi.org/10.7324/JAPS.2019.90817.

Karthikeyan, R., Karempudi, B., Rasheed, S. and Vijayaraj, P. (2012), "Dendritic architechture for the delivery of antibacterial agent against resistant producing strains", *Cent. Euro. J. Exp. Bio.*, **1**, 45-48.

Khosroshahi, A.G., Amanlou, M., Sabzevari, O., Daha, F.J., Aghasadeghi, M.R., Ghorbani, M., Ardestani, M.S., Alavidjeh, M.S., Sadat, S.M., Pouriayevali, M.H. and Mousavi, L. (2013), "A comparative study of two novel nanosized radiolabeled analogues of methionine for SPECT tumor imaging", *Curr. Med. Chem.*, **20**(1), 123-133.

Kung, M.P., Stevenson, D.A., Plössl, K., Meegalla, S.K., Beckwith, A., Essman, W.D., Mu, M., Lucki, I. and Kung, H.F. (1997), "[^{99m}Tc] TRODAT-1: A novel technetium-99m complex as a dopamine transporter imaging agent", *Eur. J. Nucl. Med.*, **24**(4), 372-380. https://doi.org/10.1007/BF00881808.

Lambrecht, F.Y. (2011), "Evaluation of ^{99m}Tc-labeled antibiotics for infection detection", *Annal. Nucl. Med.*, **25**(1), 1-6. https://doi.org/10.1007/s12149-010-0417-3.

Li, C., Cao, X., Ma, Z., Sun, X., Hu, F. and Wang, L. (2018), "Effect of pre-surgery assessments on the prognosis of patients received extracranial-intracranial bypass surgery", *Restor. Neurol. Neuros.*, **36**(5), 593-604. https://doi.org/10.3233/RNN-180848.

Lupetti, A., Welling, M.M., Pauwels, E.K. and Nibbering, P.H. (2003), "Radiolabelled antimicrobial peptides for infection detection", *Lancet Infect. Dis.*, **3**(4), 223-229. https://doi.org/10.1053/j.semnuclmed.2017.11.003.

Madavan, R. and Balaraman, S. (2017), "Investigation on effects of different types of nanoparticles on critical parameters of nano-liquid insulation systems", *J. Mol. Liq.*, **230**, 437-444. https://doi.org/10.1109/ICDL.2019.8796708.

Mäkinen, T.J., Lankinen, P., Pöyhönen, T., Jalava, J., Aro, H.T. and Roivainen, A. (2005), "Comparison of 18 F-FDG and 68 Ga PET imaging in the assessment of experimental osteomyelitis due to Staphylococcus aureus", *Eur. J. Nucl. Med. Mol. I.*, **32**(11), 1259-1268. https://doi.org/10.1007/s00259-005-1841-9.

Magneson, G.R. and Orahood, R.C. (2016), "Compositions for radiolabeling diethylenetriaminepentaacetic acid (DTPA)-dextran", U.S. Patent, **9**, 439, 985.

Miyashita, H., Nakahara, T., Asoda, S., Kameyama, K., Kawaida, M., Enomoto, R., Shiba, H., Jinzaki, M., Kawana, H. and Nakagawa, T. (2019), "Clinical value of 3D SPECT/CT imaging for assessing jaw bone invasion in oral cancer patients", *J. Cranio-Maxill. Surg.*, **47**(7), 1139-1146. https://doi.org/10.1016/j.jcms.2019.03.013.

Mohtavinejad, N., Amanlou, M., Bitarafan-Rajabi, A., Pormohammad, A. and Ardestani, M.S. (2020), "Technetium-99 m-PEGylated dendrimer-G2-(Dabcyle-Lys6, Phe7)-pHBSP: A novel Nano-Radiotracer for molecular and early detecting of cardiac ischemic region", *Bioorg. Chem.*, **45**(6), 10373. https://doi.org/10.1016/j.bioorg.2020.103731.

Okarvi, S.M. (2004), "Erratum: Peptide-based radiopharmaceuticals: Future tools for diagnostic imaging of cancers and other diseases", *Med. Res. Rev.*, **24**(5), 685-686. https://doi.org/10.1002/med.20015.

Pakos, E.E., Trikalinos, T.A., Fotopoulos, A.D. and Ioannidis, J.P. (2007), "Prosthesis infection: diagnosis after total joint arthroplasty with antigranulocyte scintigraphy with ^{99m}Tc-labeled monoclonal antibodie−A meta-analysis", *Radiology*, **242**(1), 101-108. https://doi.org/10.1148/radiol.2421052011.

Raza, M.A., Kanwal, Z., Rauf, A., Sabri, A.N., Riaz, S. and

Naseem, S. (2016), "Size-and shape-dependent antibacterial studies of silver nanoparticles synthesized by wet chemical routes", *Nanomaterials*, **6**(4), 74. https://doi.org/10.3390/nano6040074.

Roohi, S., Mushtaq, A. and Malik, S.A. (2005), "Synthesis and biodistribution of 99mTc-Vancomycin in a model of bacterial infection", *Radiochim. Acta.*, **93**(7), 415-418. https://doi.org/10.1524/ract.2005.93.7.415.

Roohi, S., Mushtaq, A., Jehangir, M. and Malik, S.A. (2006), "Synthesis, quality control and biodistribution of ^{99m}Tc-Kanamycin", *J. Radioanal. Nucl. Ch.*, 267(3), 561-566. https://doi.org/10.1007/s10967-006-0087-8.

Sadeek, S.A. and El-Hamid, S.M.A. (2016), "Synthesis, spectroscopic, thermal analysis and in vitro biological properties of some new metal complexes with gemifloxacin and 1, 10-phenanthroline", *J. Therm. Anal. Calorim.*, **124**(1), 547-562. https://doi.org/10.1007/s10973-015-5057-3.

Shahzad, S., Qadir, M.A., Rasheed, R. and Ahmed, M. (2019), "Synthesis of 99mTc-gemifloxacin freeze dried kits and their biodistribution in Salmonella typhi, Pseudomonas aeruginosa and Klebsiella pneumoniae", *Arab. J. Chem.*, **12**(5), 664-670. https://doi.org/10.1016/j.arabjc.2015.10.002.

Sharma, R., Kim, S.Y., Sharma, A., Zhang, Z., Kambhampati, S.P., Kannan, S. and Kannan, R.M. (2017), "Activated microglia targeting dendrimer–minocycline conjugate as therapeutics for neuroinflammation", *Bioconjugate Chem.*, **28**(11), 2874-2886. https://doi.org/10.1021/acs.bioconjchem.7b00569.

Signore, A. and Glaudemans, A.W. (2011), "The molecular imaging approach to image infections and inflammation by nuclear medicine techniques", *Annal. Nucl. Med.*, **25**(10), 681-700. https://doi.org/10.1007/s12149-011-0521-z.

Solanki, K.K., Bomanji, J., Siraj, Q., Small, M. and Britton, K.E. (1993), "^{99m}Tc Infecton−A new class of radiopharmaceutical for imaging infection", *J. Nucl. Med.*, **34**, 119A.

Sonvico, F., Clementino, A., Buttini, F., Colombo, G., Pescina, S., Stanisçuaski Guterres, S., Raffin Pohlmann, A. and Nicoli, S. (2018), "Surface-modified nanocarriers for nose-to-brain delivery: from bioadhesion to targeting", *Pharmaceutics*, **10**(1), 34. https://doi.org/10.3390/pharmaceutics10010034.

Torres, L., Alves, V., Oliveira, A. and Pereira, J. (2018), "Fab'fragments of ^{99m}Tc-labeled anti-granulocyte monoclonal antibodies in vascular graft infection", *Annal. Nucl. Med.*, **15**(10), 621-627.

Yurt Lambrecht, F., Yilmaz, O., Unak, P., Seyitoglu, B., Durkan, K. and Baskan, H. (2008), "Evaluation of ^{99m}Tc- Cefuroxime axetil for imaging of inflammation", *J. Radioanal. Nucl. Chem.*, **277**(2), 491-494. https://doi.org/10.1007/s10967-007-7111-5.